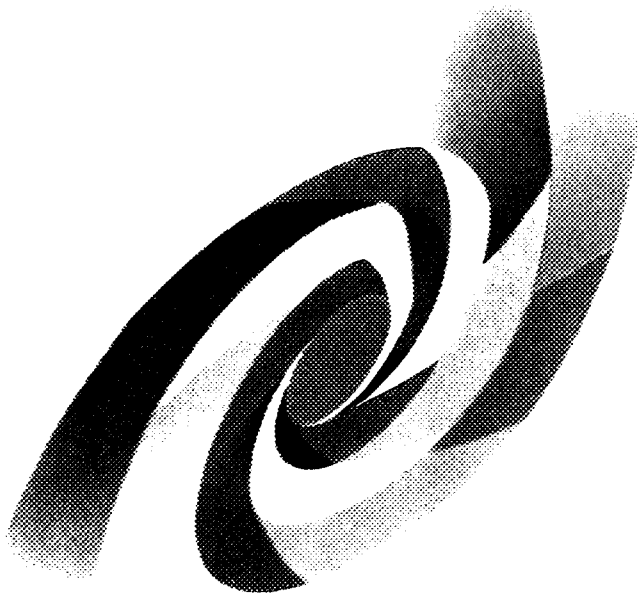
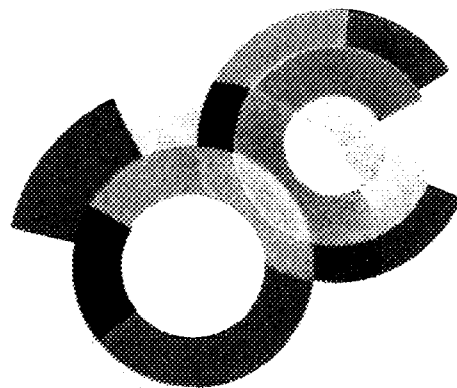
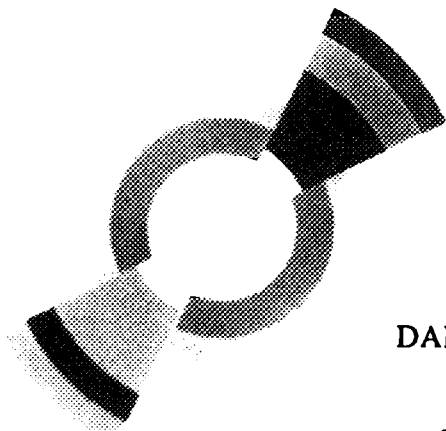




SERVICE DE PHYSIQUE DES PARTICULES



Gestion INIS
Doc. enreg. le : 16/9/96
N° TRN :
Destination : I,I+D,D



DAPNIA/SPP 96-04

February 1996

HIGHLIGHTS OF ELECTRON-PROTON DEEP INELASTIC SCATTERING AT HERA

J. Feltesse

*Contribution to the II Rencontres du Vietnam,
Ho Chi Minh City, 21-28 October 1995*

DAPNIA

29-03-

dc

Le DAPNIA (Département d'Astrophysique, de physique des Particules, de physique Nucléaire et de l'Instrumentation Associée) regroupe les activités du Service d'Astrophysique (SAp), du Département de Physique des Particules Élémentaires (DPhPE) et du Département de Physique Nucléaire (DPhN).

Adresse : DAPNIA, Bâtiment 141
CEA Saclay
F - 91191 Gif-sur-Yvette Cedex

HIGHLIGHTS OF ELECTRON-PROTON DEEP INELASTIC SCATTERING AT HERA

Joël Feltesse

DSM/DAPNIA/Service de Physique des Particules
CEA Saclay
F-91191 Gif-sur-Yvette Cedex, France

Abstract

Salient results on deep inelastic scattering from the H1 and ZEUS collaborations are reviewed. These include preliminary measurements of the proton structure function F_2 extending to new regimes at both high Q^2 and low Q^2 and x , studies of the hadronic final states and discussion on QCD interpretations of low x data. New determination of α_s from jet rates in deep inelastic scattering based on 1994 data are presented. A consistent picture of the gluon density in the proton at low x from a variety of processes is obtained.

1. Introduction

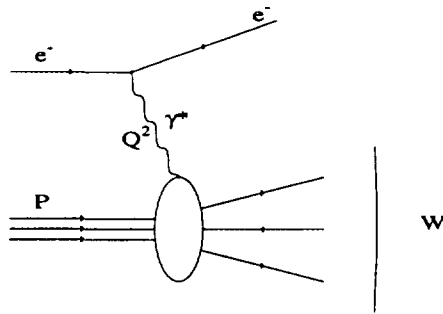


Fig. 1. Basic Feynman diagram for electron proton deep inelastic scattering. Q^2 is minus the squared four momentum transferred or minus the squared mass of the virtual photon. W is the virtual photon-proton centre of mass energy.

In Deep Inelastic lepton-nucleon Scattering (DIS) at HERA Q^2 , minus the squared four-momentum of the exchanged virtual photon (Fig.1), can reach 90000 GeV^2 , a value more than 100 times larger than achieved in fixed target experiments. May be even more important, x , the fraction of proton momentum carried by the struck quark can be as low as $5 \cdot 10^{-5}$ at Q^2 values $\leq 4 \text{ GeV}^2$. The low x regime is a new domain of test for QCD. At sufficiently low x values, in perturbative calculations resummations based on leading $(\alpha_s \log(Q^2/Q_0^2))^n$ terms, the so-called Dokshitzer Gribov Lipatov Altarelli Parisi (DGLAP) mechanism ¹ should eventually be superseded by resummations based on leading $(\alpha_s \log 1/x)^n$ terms, the so-called Balitski Fadin Kuraev Lipatov (BFKL) mechanism ². In this review we present the most recent results on the structure function $F_2(x, Q^2)$ of the proton and then discuss how these data together with less inclusive measurements can give insight into the QCD underlying mechanism at low x . We show how studies of the jets in deep inelastic scattering can provide new determinations of the coupling constant $\alpha_s(Q^2)$ and a direct measurement of the gluon density in the proton. The measurement of the gluon density is compared to determinations in other processes.

2. The proton structure function $F_2(x, Q^2)$

The first determination ^{3,4} of the proton structure function $F_2(x, Q^2)$ at HERA in 1992 has been based on a recorded luminosity of about 30 nb^{-1} and has revealed the striking feature of a proton structure function rising as x decreases below 10^{-2} , for Q^2 values in the range $8 < Q^2 < 60 \text{ GeV}^2$. The analysis of the 1993 data based on 10 to 20 times more integrated luminosity reported by the H1 ⁵ and ZEUS ⁶ collaborations extends the kinematic range to a lower Q^2 value of 4.5 GeV^2 and to larger Q^2 values up to 2000 GeV^2 . The 1994 data represents a further increase of about a factor 10 in statistics at large Q^2 together with an extension of the accessible kinematic range towards $Q^2 = 1 \text{ GeV}^2$ and $x = 0.00005$.

Access to such low Q^2 values has been achieved by two different ways : first by operating HERA for two days with the interaction point shifted to the proton direction ^{10,11} to improve acceptance at low scattering angle, second by selecting events from the nominal interaction point but where a photon has been emitted collinear with the electron beam, thus reducing the effective electron beam energy ¹².

At very high $Q^2 \geq 5000 \text{ GeV}^2$ the number of recorded events is so far too meager to extract structure functions of neutral or charge currents. Data at high Q^2 are however very sensitive to new phenomena. By comparing the measured differential cross section $d\sigma/dQ^2$ with the expected cross section from the Standard Model, the HERA experiments have provided new limits on masses and couplings of leptoquarks and on fermion compositeness scales. For example, based on data recorded

in 1993 and 1994, compositeness scales smaller than 1.0 TeV to 2.5 TeV, pending on the chiralities of the currents, can be ruled out ¹³. Direct searches on leptoquarks, supersymmetric particles, excited leptons, excited quarks have not yet been successful but provide limits comparable or even better than obtained from other colliders ^{14,15}.

2.1. Results on $F_2(x, Q^2)$

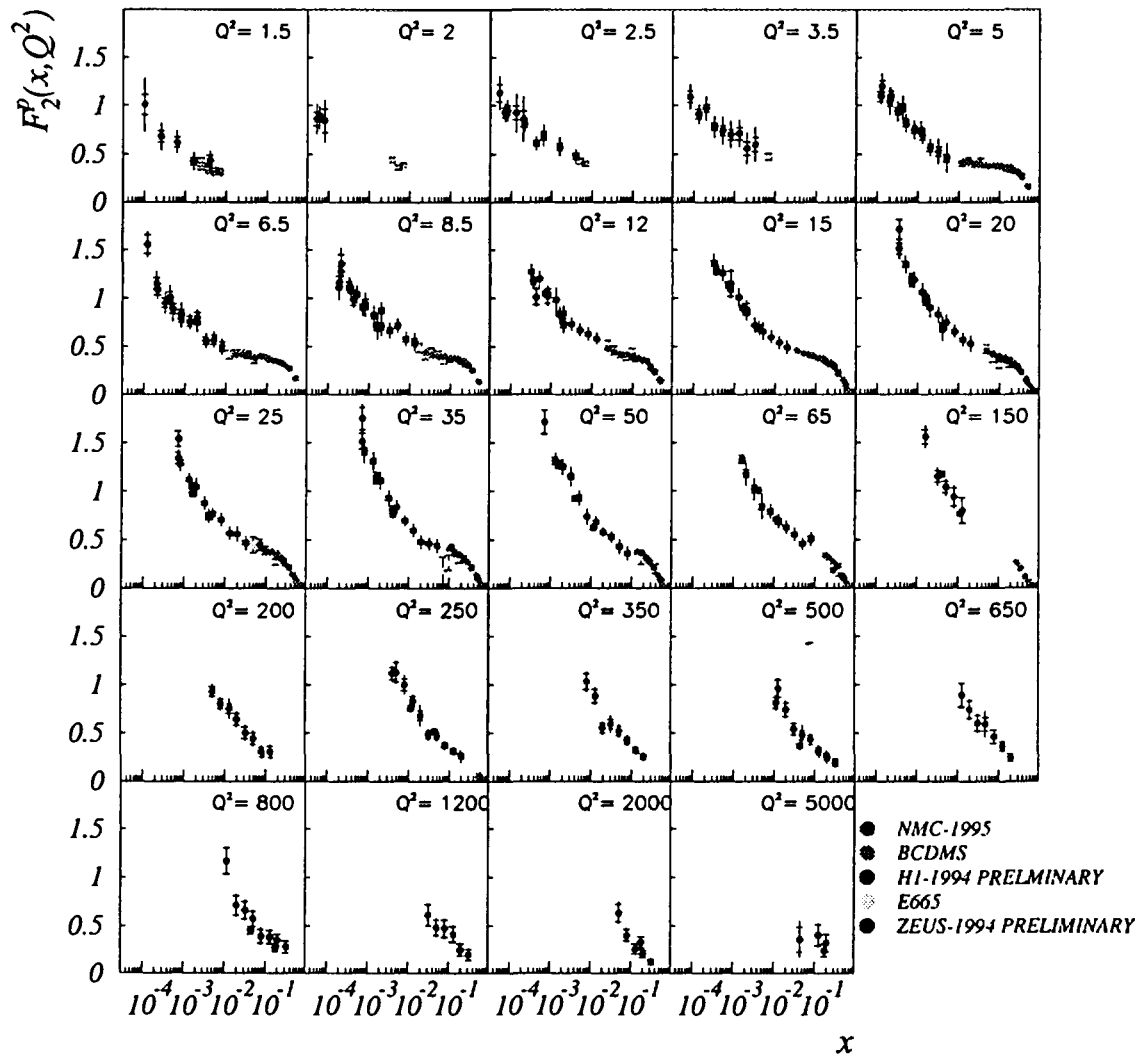


Fig. 2. Measurement of the proton structure function $F_2(x, Q^2)$ vs x for fixed values of Q^2 . Preliminary 1994 data from H1 and ZEUS are compared to the fixed target data of BCDMS, E665 and NMC.

The results on $F_2(x, Q^2)$ from H1 and ZEUS together with those of BCDMS ⁷, E665 ⁸ and NMC ⁹ are shown in Fig. 2 as a function of x at fixed Q^2 values. We can see that the x, Q^2 bins of the H1 data have closed the kinematical gap between the fixed target data of E665 and the HERA results. The preliminary H1 data cover the full 1994 data set whereas the ZEUS data are so far restricted to the low Q^2 shifted interaction point data and data points at very high Q^2 . The preliminary results of 1994 data have still systematics of about 10 % but there is a reasonable hope to decrease the systematics down to 5 % in the final data from the nominal interaction point. The normalisation errors in the large statistics 1994 H1 data sample taken with HERA nominal conditions has become

almost negligible. It has been reduced to 1.5%.

In all the bins where the comparison is possible the data sets of H1 and ZEUS agree well within the errors. There is also a smooth transition between the fixed target data and the HERA data. It is remarkable that the steep rise of F_2 with x decreasing persists to Q^2 values as low as 1.5 GeV^2 at $x < 10^{-2}$ and is already visible at $Q^2 = 2000 \text{ GeV}^2$ at $x \sim 0.1$. At a fixed low x value, for example $x = 10^{-3}$, the steepness increases with Q^2 increasing.

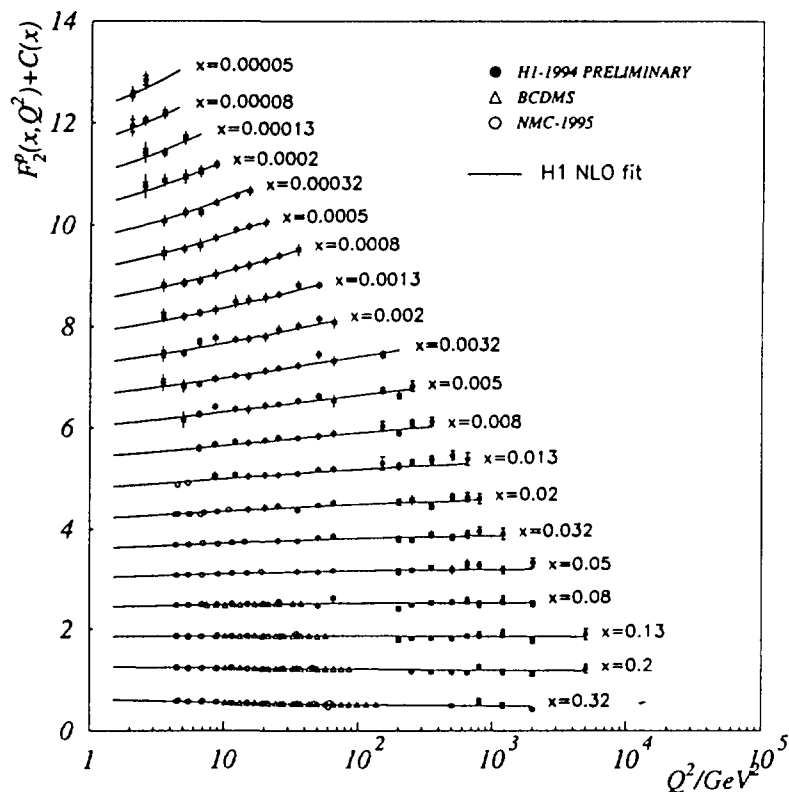


Fig. 3. Measurement of the proton structure function $F_2(x, Q^2)$ vs Q^2 for fixed values of x . Preliminary 1994 data from H1 (closed points) are compared to the fixed target data of BCDMS (open triangles) and NMC (open circles). The curves represent the DGLAP NLO QCD fit described in the text. For clarity the F_2 values are plotted, with all but normalisation errors, adding a term $c(x) = 0.6(i_x - 0.5)$ to F_2 , where i_x is the bin number starting at $i_x = 1$ for $x = 0.32$.

The H1 1994 data are shown in Fig. 3 together with the data of BCDMS and NMC as a function of Q^2 at fixed x values. Here also the H1 data agree well with a smooth extrapolation from NMC and BCDMS data. As in the fixed target domain, there are no scaling violations at $x \sim 0.1$, but pronounced Q^2 scaling violations at low x , steeper with x decreasing towards $x = 0.00005$.

2.2. QCD interpretation

It was not known before data from HERA have become available whether some strong non perturbative effects would not mask the asymptotic behaviour anticipated in the early days of QCD ¹⁶. The observation of the steep rise of F_2 at low x is a success of QCD as an asymptotic free field theory.

The two salient features of the data at low x , the rise of F_2 as x decreases and the strong scaling violations, can be interpreted in perturbative QCD. The H1 collaboration has made a common fit of the 1994 preliminary data at $Q^2 > 5 \text{ GeV}^2$ together with the new NMC data and the BCDMS measurements. The fit is based on Next-to-Leading Order (NLO) DGLAP evolution equations and it gives a very good description of the data not only at $Q^2 > 5 \text{ GeV}^2$ but also surprisingly down to

$Q^2 = 1.5 \text{ GeV}^2$ and $x = 0.00005$ (see Fig.3). Similar fits have been made on ZEUS and H1 1993 data combined with fixed target data ^{17,18,19,20}. All the fits require a starting distribution at $Q_0^2 = 4 \text{ GeV}^2$ to be singular in $x^{-\lambda}$, with $\lambda \sim 0.2$ to 0.4 , when x goes to zero. The fits give a satisfying description of the data, demonstrating that, within the present size of the errors, the DGLAP evolution equations are still valid in the HERA low x kinematic domain (see Fig.4). The fits have been used to determine the gluon density in the proton at very low x ²⁰ (see section 3.2.2).

The H1 collaboration has also used the BFKL evolution equation as a further constraint at low x ²⁰. The quality of the fit is neither improved nor deteriorated. There is at present clearly no need for the BFKL mechanism to describe the Q^2 evolution of the data. With more precise data it will be possible to investigate the behaviour of the slope $dF_2/d\log(1/x)$, a variable very sensitive to the underlying mechanisms ²¹.

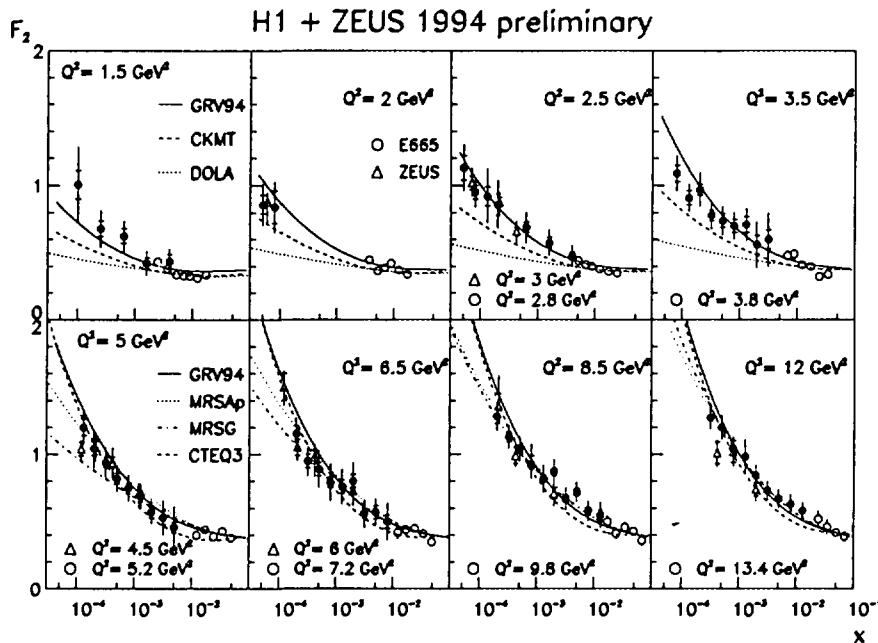


Fig. 4. Measurement of the structure F_2 in the low Q^2 region of H1 (solid points), ZEUS (open triangles) and from the muon experiment E665 (open circles). The data are compared to different parton parametrizations at $Q^2 < 5 \text{ GeV}^2$ the Regge inspired DOLA and CKMT, at $Q^2 > 5 \text{ GeV}^2$ the global fits MRSx and CTEQ3, and for the whole Q^2 range the GRV.

An alternative way to test that the rise of F_2 at low x is entirely due to the perturbative QCD evolution has been developed by Glück, Reya and Vogt (GRV) ²². At a very low $Q_0^2 = 0.34 \text{ GeV}^2$ value valence-like parton distributions are used as input to the DGLAP evolution equations. This yields a parametrisation of the structure function F_2 which is in accord with the data down to $Q^2 = 1.5 \text{ GeV}^2$ (see Fig.4). It demonstrates that the DGLAP evolution equations are not only capable to describe the Q^2 evolution but also capable to generate the rise of F_2 with x decreasing provided a non singular input distribution is used at a very low Q^2 scale. This is in contrast to a Regge model ²³ without Q^2 evolution, referred to as DOLA in Fig.4, which is found not to describe the data even at the lowest Q^2 values at 1.5 GeV^2 . A model ²⁴, referred to as CKMT in Fig.4, inspired from Regge phenomenology up to $Q^2 = 2 \text{ GeV}^2$ and based on DGLAP evolution at higher Q^2 values is closer to the data although not fully satisfying.

3. The hadronic final state in DIS events

At moderate $x \geq 0.01$ values DIS events are a copious source of jets well described by the DGLAP

mechanism, from which the coupling constant $\alpha_s(Q^2)$ and the gluon density in the proton can be extracted (see section 3.2). At lower x values, hadron production in the region between the current jet and the proton remnant is expected to be sensitive to the effects of the BFKL or DGLAP dynamics (Fig.5).

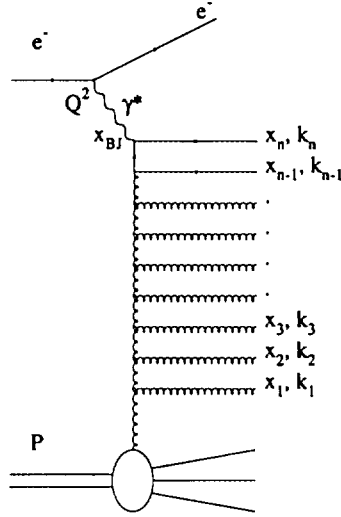


Fig. 5. Diagrammatic representation of the gluon rungs contributing to deep inelastic scattering.

3.1. BFKL versus DGLAP dynamics

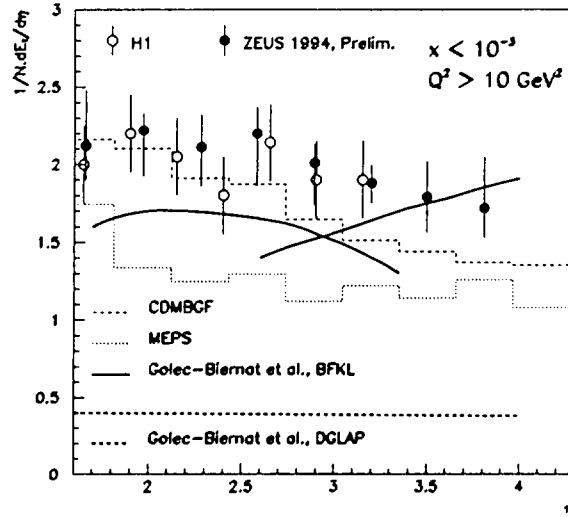


Fig. 6. Average transverse energy measured in the forward hemisphere in the laboratory ($\eta \geq 0$) by H1 and ZEUS at low x . The data are compared to analytic QCD calculations at the parton level and to MEPS and CDMBGF full simulations.

In the DGLAP scheme, the parton cascade emitted before a quark is struck by the virtual photon (see Fig. 5) follows a soft ordering for the fractional momentum $x \leq x_n \leq \dots \leq x_2 \leq x_1$ but a strong ordering in transverse momentum $Q^2 \gg k_n^2 \gg \dots \gg k_2^2 \gg k_1^2 \gg Q_0^2$. In the BFKL scheme there is no strong ordering in transverse momentum but a strong ordering in the fractional momentum

$x \ll x_n \ll \dots \ll x_2 \ll x_1$. The phase space available is larger than for strong transverse momentum ordering. BFKL evolution is expected to produce more transverse energy E_T than DGLAP evolution. The transverse energy measured by the HERA experiments ^{25,26} (Fig. 6) is found to be much smaller than full simulations based on the DGLAP mechanism (the Matrix Element + Parton Shower model MEPS) ²⁷ and a bit smaller than analytic calculations ²⁸ performed at the parton level based on the BFKL mechanism. In the BFKL calculation, however, contributions from hadronization are not included which may add about 0.5 GeV to the parton transverse energy. In contrast to the MEPS model, the CDMBGF model ²⁹ (Colour Dipole Model plus Boson Gluon Fusion) gives a fair description of the data. In this model, gluon emission is similar to that of BFKL emission because the gluons emitted do not obey a strong ordering in transverse momentum.

The measured rate of forward jets ³⁰ in DIS events at very low x provides similar hints on the failure of the MEPS model and the success of BFKL-like calculations to describe the hadronic final state between the current jet and the proton remnant. In the absence of full simulations based on BFKL dynamics no firm conclusion can be drawn yet. The study of possible signatures of BFKL mechanism in the hadronic final state looks promising at very low x .

3.2. Jet rates in DIS events

The hadronic final state of deep inelastic events is also a copious source of jets. Radiation of hard gluon from the initial or struck quark, also called QCD-Compton ($\gamma^*q \rightarrow gq$), or production of a quark anti-quark pair by photon-gluon fusion ($\gamma^*g \rightarrow q\bar{q}$) are expected to produce $(2 + 1)$ jets (2 high p_t jets and the proton remnant) in the hadronic final state of DIS events. The production rate is a simple function of $\alpha_s(Q^2)$ and of the gluon density in the proton. With very large statistics it should be possible to fit simultaneously these two quantities. So far, the data have been integrated over x to extract $\alpha_s(Q^2)$ and integrated over Q^2 to extract the gluon density as a function of x .

3.2.1. α_s measurement

At $x \geq 0.01$, simulations based on the MEPS model give an excellent description of the energy flow in multi-jet events ³¹ (see Fig. 7).

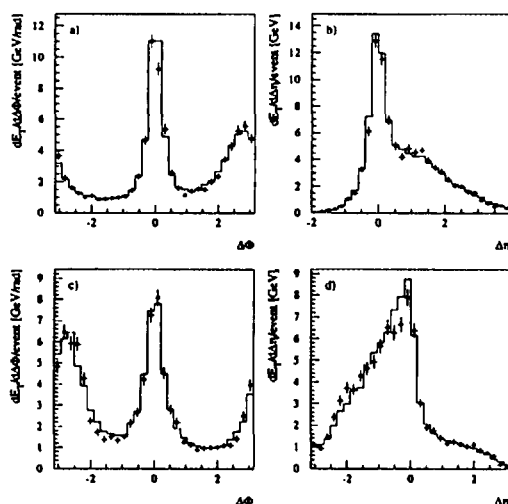


Fig. 7. The transverse energy flow in the laboratory frame as a function of a) $\Delta\Phi$ and b) $\Delta\eta$ for the most backward going jet and c) and d) for the most forward going jet using the jet axis as reference. The points represent the jet data sample and the errors are statistical. The histogram gives the predictions of the MEPS model.

It is a domain of x where the quark and gluon densities are well known from the fixed target experiments. The measured (2+1)-jet rate of events has been corrected at the parton level to be compared with a NLO theoretical calculation to determine α_s in three Q^2 intervals. A combined fit of the six determinations by the H1³¹ and ZEUS³² experiments extrapolated to the mass of the Z particle provides the following average

$$\alpha_s(M_Z) = 0.120 \pm 0.005 \pm 0.007 \quad (1)$$

where the first error involves statistical and systematic errors non correlated between the two experiments and the second error is the quadratic average of common theoretical errors.

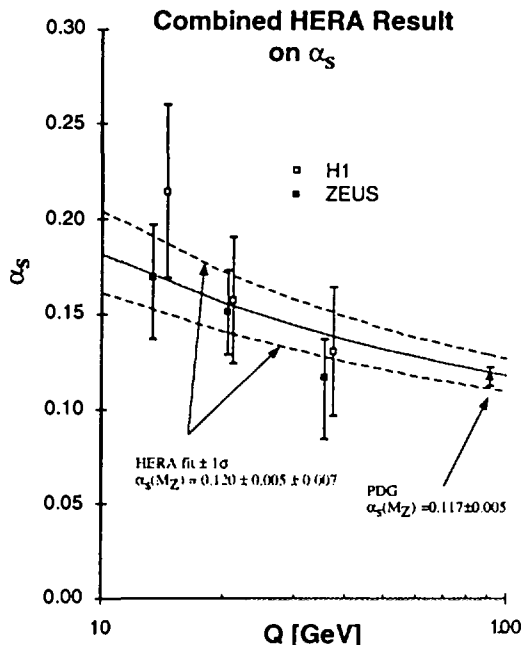


Fig. 8. The measured value of α_s from the rate of (2+1)-jet events as a function of Q^2 . The data points are from H1 and ZEUS. The line presents the combined result of the two experiments with the 1σ total error band. For comparison the world average at the Z mass is also plotted.

3.2.2. Gluon density

The H1 Collaboration has also provided a first direct determination of the gluon density in the proton³³. The analysis is based on the data sample accumulated in 1993 (242 nb^{-1}). In a (2+1)-jet photon-gluon fusion event it is possible to reconstruct the fraction of the proton momentum carried by the gluon $x_{g/p} = x(1 + \hat{s}/Q^2)$ where \hat{s} is the two-jet invariant mass. In the kinematic range defined as $0.0003 < x < 0.0015$ and $0.002 < x_{g/p} < 0.2$, 75 % of the (2+1)-jet events are due to the photon gluon fusion process. The remained 25 % of events are due to QCD Compton processes and can be statistically subtracted. The resulting LO gluon distribution is shown in figure 9 as a function of $x_{g/p}$ at an average Q^2 value of 30 GeV^2 . The measurement is compared to recent indirect determinations from the scaling violations of the structure function F_2 at very low x by the H1³⁴ and ZEUS³⁵ experiments or obtained in global parametrisations of LO parton densities^{22,18}. The HERA data are also compared to a determination from the NMC experiment based on inelastic J/Ψ determination at $x \geq 0.01$. The overall consistency between direct and indirect determinations is a remarkable non trivial success of QCD.

4. Conclusion

In summary HERA data on the proton structure function and on the hadronic final state in DIS events have already brought important insight into the underlying QCD mechanisms at low x . From

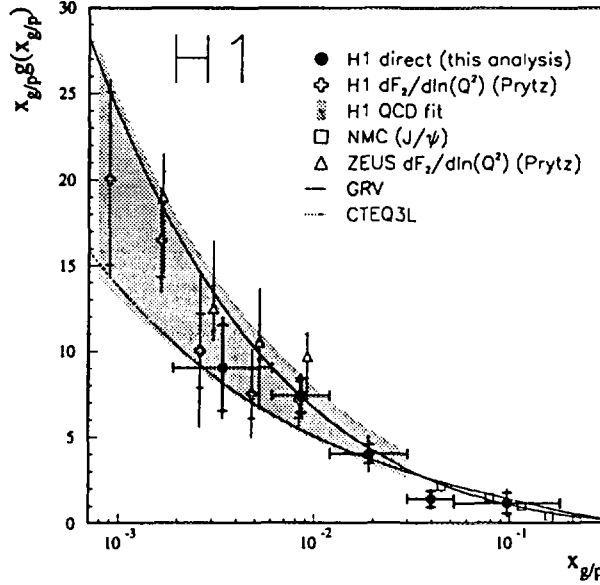


Fig. 9. The gluon density at $\langle Q^2 \rangle = 30 \text{ GeV}^2$ as a function of the fraction of the proton momentum carried by the gluon. The H1 points from jet-multiplicity are compared with indirect determinations by H1 and ZEUS at $Q^2 = 20 \text{ GeV}^2$ and by NMC from J/Ψ production evolved to $Q^2 = 30 \text{ GeV}^2$.

the jet multiplicity competitive determinations of the gluon density and of α_s , have been obtained. The analysis of the special class of DIS events where the struck proton stays intact after the interaction is covered in another talk ³⁷. A discussion of photoproduction at HERA can also be found in these proceedings ³⁶. These beautiful results only represent a part of HERA physics. Important topics as production of heavy quarks and vector mesons, fragmentations and detailed searches beyond the Standard Model have been omitted. A new field of HERA physics on rare events and at high Q^2 will be open as the HERA luminosity will increase.

5. Acknowledgements

I would like to thank Professor Tran Thanh Van and all the organisers of the Second Rencontres du Vietnam for the very pleasant atmosphere to establish fruitful contacts between particle physicists and astrophysicists and between Vietnamese physicists and physicists from all over the world. Many thanks to A. De Roeck and G. Cozzika for help preparing this manuscript.

1. V.N. Gribov and L.N. Lipatov, *Sov. J. Nucl. Phys.* **15** (1972) 438 and 675;
G. Altarelli and G. Parisi, *Nucl. Phys.* **B126** (1977) 298 ;
Yu.L. Dokshitzer, *Sov. Phys. JETP* **46** (1977) 641.
2. E.A. Kuraev, L.N. Lipatov and V.S. Fadin, *Phys. Lett.* **B60** (1975) 50 ;
Ya. Ya. Balitski and L.N. Lipatov, *Sov. J. Nucl. Phys.* **28** (1978) 822 and *Zh. Eksperiment. I. Teor. Fiz.* **72** (1977) 377.
3. H1 Collaboration, I. Abt et al., *Nucl. Phys.* **B407** (1993) 515.
4. ZEUS Collaboration, M. Derrick et al., *Nucl. Phys.* **B316** (1993) 412.
5. H1 Collaboration, T. Ahmed et al., *Nucl. Phys.* **B439** (1995) 471.
6. ZEUS Collaboration, M. Derrick et al., *Z. Phys.* **C65** (1995) 379.
7. BCDMS Collaboration, A.C. Benvenuti et al., *Phys. Lett.* **B223** (1989) 485.
8. E-665 FNAL Collaboration, A. Kotwal, preprint FERMILAB-CONF-95-046-E and pro-

- ceedings of the *XXXth Rencontres de Moriond*, 19-25 Mars 1995.
9. NMC Collaboration, M. Arneodo et al., preprint **CERN-PPE/95-138**.
 10. H1 Collaboration, **EPS-0470** and U. Strauman, proceedings of the *EPS-HEP95 Conference*, Brussels, 1995 and G. Bernardi, these proceedings.
 11. ZEUS Collaboration, M. Derrick et al., preprint **DESY 95-193**; A. Caldwell proceedings of *XVII International Symposium on Lepton Photon Interactions*, Beijing, China, August 1995.
 12. H1 Collaboration, **EPS-0472** and U. Strauman, proceedings of the *EPS-HEP95 Conference*, Brussels, 1995.
 13. H1 Collaboration, S. Aid et al., *Phys. Lett.* **B353** (1995) 578.
 14. H1 Collaboration, S. Aid et al., preprint **DESY 95-233**, contributions **EPS-0463**, **EPS-0464**, **EPS-0784** to the *EPS-HEP95 Conference*, Brussels, 1995.
 15. ZEUS Collaboration, M.Derrick et al., Contribution **EPS-0373** to the *EPS-HEP95 Conference*, Brussels, 1995.
 16. A. De Rujula et al., *Phys. Rev.* **D10** (1974) 1649.
 17. A.D. Martin, R.G. Roberts and W.J. Strirling, preprint **RAL 95-021** (1995)
 18. CTEQ Collaboration, H.L. Lai et al. *Phys. Rev.* **D51** (1995) 4763.
 19. ZEUS Collaboration, M. Derrick et al., *Phys. Lett.* **B345** (1995) 576.
 20. H1 Collaboration, S. Aid et al., *Phys. Lett.* **B354** (1995) 494.
 21. H. Navelet, R. Peschanski and S. Wallon, *Mod. Phys. Lett.* **A9** (1994) 3393.
 22. M. Glück, E. Reya and A. Vogt, *Z. Phys.* **C67** (1995) 433.
 23. A. Donnachie and P.V. Landshoff, *Z. Phys.* **C61** (1994) 139.
 24. A. Capella et al., *Phys. Lett.* **B337** (1994) 358.
 25. H1 Collaboration, I. Abt et al., *Z. Phys.* **C63** (1994) 377.
 26. ZEUS Collaboration, M.Derrick et al., Contribution **EPS-0391** to the *EPS-HEP95 Conference*, Brussels, 1995.
 27. G. Ingelman, Proceedings of the Workshop on Physics at HERA, Hamburg 1991, vol.3, p.1366.
 28. K. Golec-Biernat et al., *Phys. Lett.* **B335** (1994) 220.
 29. L. Lönnblad, *Comp. Phys. Comm.* **71** (1992) 15.
 30. H1 Collaboration, S. Aid et al., *Phys. Lett.* **B356** (1995) 118.
 31. H1 Collaboration, Contribution **EPS-0486** to the *EPS-HEP95 Conference*, Brussels, 1995.
 32. ZEUS Collaboration, M.Derrick et al., preprint **DESY 95-182**.
 33. H1 Collaboration, S. Aid et al., *Nucl. Phys.* **B449** (1995) 3.
 34. H1 Collaboration, S. Aid et al., *Phys. Lett.* **B354** (1995) 494 and Th. Naumann, these proceedings.
 35. ZEUS Collaboration, M. Derrick et al., *Phys. Lett.* **B345** (1995) 576.
 36. A. Rostovtsev, these proceedings.
 37. B. Löhr, these proceedings.